IEEE Access
Multidisciplinary | Rapid Review | Open Access Journal

Received June 14, 2018, accepted July 13, 2018, date of publication July 25, 2018, date of current version August 20, 2018.

Digital Object Identifier 10.1109/ACCESS.2018.2859803

Experimental Investigation on the Interaction Mechanism Between Microwave Field and Semiconductor Material

YONG GAO[1], EN LI[1,2], (Member, IEEE), GAOFENG GUO[1], AND HU ZHENG[1]
[1]School of Electronic Science and Engineering, University of Electronic Science and Technology of China, Chengdu 611731, China
[2]National Engineering Research Center of Electromagnetic Radiation Control Materials, University of Electronic Science and Technology of China, Chengdu 611731, China

Corresponding author: Yong Gao (gy_eee@163.com)

This work was supported by the National Natural Science Foundation of China under Grants 61671123 and 61001027.

ABSTRACT An experimental method and apparatus for investigating the interaction mechanism between microwave field and semiconductor material are presented in this paper. The investigation is based on a dual-mode compressed rectangular cavity, which includes the TE_{102} and TE_{103} modes. The TE_{102} mode is used for providing the stimulus signal, which supplies the microwave field during the experiment, and the TE_{103} mode is for testing. The two modes are individually coupled to the cavity, and two band-stop filters are introduced to isolate the signals coming from both the modes. A directional coupler is utilized to monitor the power level of the stimulus signal. Experimental results demonstrate that microwave field may affect the inherent characteristics of indium phosphate, a typical kind of semiconductor materials, which eventually leads to the nonlinear behavior of the dielectric property. After the microwave field strength exceeds a critical value, the nonlinear behavior of the microwave materials becomes more and more drastic along with further increasing field strength, and according to the particular experiment setup, we conclude that the nonlinear behavior is not caused by microwave thermal effect, but some inherent characteristics of the material itself. In addition, the experimental method and apparatus can also be employed to predict the consequences of the non-thermal action of microwave effect of other high-power microwave material under microwave field.

INDEX TERMS Microwave cavity, microwave field, measurement, nonlinear dielectric.

I. INTRODUCTION

It is of great importance to get access to the accurate dielectric value of microwave materials for implementing microwave circuits and systems [1]. In particular, the stability of the dielectric property of the microwave materials under a special applied environment directly affects the performances of the microwave circuits and systems. Nowadays, the microwave circuit moves towards miniaturization and integration. Meanwhile, the application of high power microwave technology is covering a lot of areas consistently and rapidly. The above factors result in the significant increase of the microwave field in the microwave substrate materials. Therefore, many microwave researchers have paid their attention to explore the dielectric property of material under strong microwave field [2]–[14].

The interaction mechanism between microwave field and materials is still unclear, even though microwave heating is considered to be the main contributes. However, a large number of reports have demonstrated the non-thermal effect is definitely exist [3]–[7]. It was demonstrated in [3] that the microwave non-thermal effect can be used to change the structure characteristic of semiconductor materials. An increase in the conductivity of pentacene, a kind of organic semiconductor materials, was found when exposed to ionizing radiation which is a controlled method of doping the organic semiconducting materials [4]. In [5], the influence of the applied field on the resistivity of 6 H-SiC is explored when the ambient temperature is controlled. When the ambient temperature is less than 450 K, the field influence is relative small, however, when the temperature over 500 K, the field influence increase significantly. In [6], by applying the microwave field, the rate of organic compounds removal increased twice as much in comparison to the control reactor, but the temperature changes no more than 1.3 $^\circ C$.

The non-heating effect is proposed to get a much faster chemical reactions rates than the conventional synthesis at the same temperature in [7].

As one of foundation material for the development of the high power microwave devices, high-speed integrated circuit and optical fiber communication, indium phosphate (InP) has received a widespread attention [15]–[21]. Heavy ion is reported to change the structure of material [19], which may affect the physical property of the material [20], [21] and this finally results in catastrophic failures of the devices and finished system. However, with the increasing density of modern circuit and the increasing popularity of high power microwave technology, the field strength around the material is strong enough to arouse the attention of the material designer and user. Contrary to the effect of ionizing radiation on semiconductor materials, much less attention has been addressed to the influence of microwave field radiation [22]–[24].

The cavity perturbation technique is the most common resonator-based approach for measurements of low loss materials in the microwave band [25], [26]. In this paper, a dual-mode compressed rectangular cavity is developed to investigate the interaction mechanism between microwave field and semiconductor material. The TE_{102} mode is utilized to adjust the strength of microwave field, while the dielectric performance of the tested materials is monitored by TE_{103} mode. The variations of the dielectric properties of InP sample is clearly detected in the experiment after the applied microwave field exceeds a critical value. What's more, the tested materials show a significant nonlinear behavior under a larger microwave field. And the dielectric property variation becomes more and more intense with the enhancement of the field.

II. MICROWAVE CAVITY DESIGN AND ELECTRIC FIELD STRENGTH CALCULATION

A. MICROWAVE CAVITY DESIGN

A compressed rectangular cavity is designed through compressing the narrow side of a standard rectangular cavity, which has two dominant modes, TE_{102} and TE_{103}. TE_{102} mode is used to produce microwave electric fields of different strengths through adjusting the power level of the stimulus signal and TE_{103} mode detects the dielectric performance of the material by monitoring the transmission curves of the cavity. The two modes signals are coupled to the cavity individually. Fig. 1 shows the schematic of the dual-mode compressed rectangular cavity. By adjusting the length of the cavity, the TE_{102} and TE_{103} modes operate at the frequency around 2.45 GHz and 3.30 GHz respectively. The optimized cavity parameters are list as: L = 155 mm, width = 83.36 mm, height = 43.18 mm, d = 10 mm.

The compressed rectangular cavity is modeled in HFSS, as is shown in Fig. 2. Apparently, the strongest electric field of TE_{102} mode lies at L/4 and 3*L/4 of the cavity, while the strongest electric field of TE_{103} mode lies at L/6, 3*L/6 and 5*L/6 of the cavity. Additionally, the compressed region has a stronger field strength than any other place in the cavity. With a proper design, a more than twice times stronger electric field is obtained at the compressed region, where we place the materials for testing.

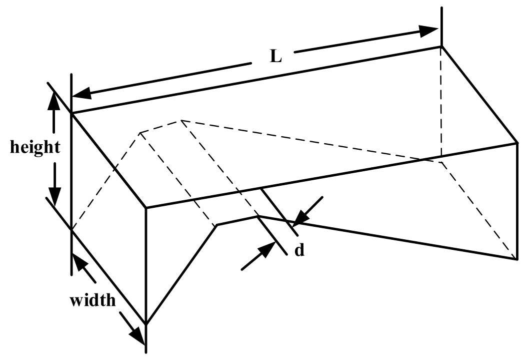

FIGURE 1. The structure schematic of the compressed cavity.

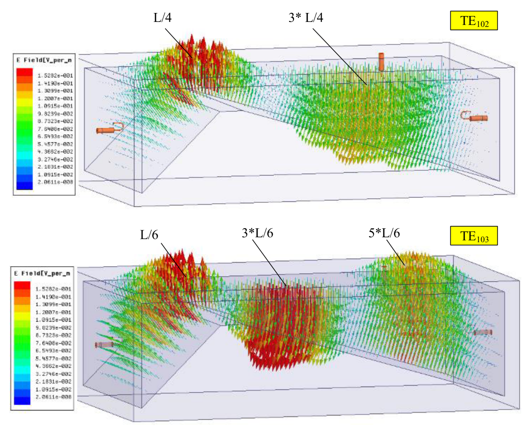

FIGURE 2. Electric field distribution of the two modes in the compressed cavity.

From Fig. 2, if the stimulus signal is injected in through a probe at the L/4 of the cavity, both of the TE_{102} and TE_{103} mode will be excited. By adjusting the power level of the stimulus signal, the electric field strength around the compressed part can be changed. Nevertheless, the stimulus port should be in a good matching condition which let the power signal be injected into the cavity well. The reflection of stimulus port of the compressed rectangular cavity is measured and shown in Fig. 3.

B. ELECTRIC FIELD STRENGTH CALCULATION THEORY

In the normal rectangular cavity, the electric fields for the TE_{102} can be written as [25],

$$
\begin{aligned}
E_y &= E_0 sin\frac{\pi x}{a} sin\frac{l\pi z}{d} \\
H_x &= \frac{-jE_0}{Z_{TE}} sin\frac{\pi x}{a} cos\frac{l\pi z}{d} \\
H_z &= \frac{j\pi E_0}{k\eta a} cos\frac{\pi x}{a} sin\frac{l\pi z}{d}
\end{aligned} \tag{1}
$$

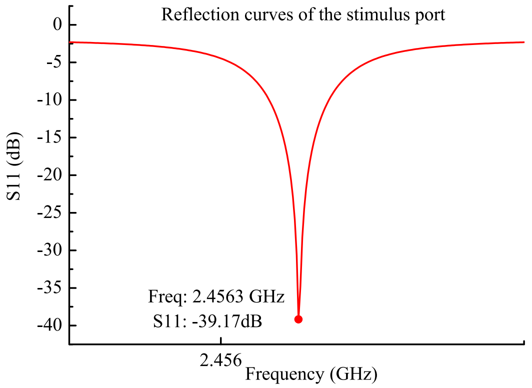

FIGURE 3. **Reflection curve of the stimulus port of the compressed cavity.**

Where E_0 is the amplitude of the electric field, Z_{TE} is wave impedance of the TE mode, η is the free space wave impedance.

Assume that there are only conductor loss in the cavity, the power of the loss can be expressed as follows:

$$P_c = \frac{R_s}{2} \int_{walls} |H_t|^2 ds \tag{2}$$

Where $R_s = \sqrt{\omega_0 \mu_0 / 2\sigma}$ is the surface resistivity of the metallic wall, and Ht is the tangential magnetic field at the surface of the wall. Using (1) in (2) gives:

$$P_c = \frac{R_s E_0^2 \lambda^2}{8\eta^2} \left(\frac{l^2 ab}{d^2} + \frac{bd}{a^2} + \frac{l^2 a}{2d} + \frac{d}{2a} \right) \tag{3}$$

When the rectangular works at the resonant frequency ω_0, the electric field energy W_e is equal to the magnetic field energy W_m,

$$W_m = W_e = \frac{\varepsilon}{4} \int_V E_y E_y^* dV = \frac{\varepsilon abd}{16} E_0^2 \tag{4}$$

With the definition of the quality factor $Q \cdot P = \omega \cdot W$ and considering, that the power P inside the resonator is related to the stimulus power P_{in} by $P = (1 - \Gamma^2) \cdot P_{in}$, where Γ is the reflection coefficient at the resonator input, we obtain the expression for the maximum electric microwave field amplitude,

$$E_0 = \sqrt{\frac{8(1 - \Gamma^2) \cdot P_{in} \cdot Q_c}{\varepsilon abd \omega_0}} \tag{5}$$

In the paper, we compress the height of the cavity at the one quarter of the wavelength place. Therefore the local electric field strength is increased greatly. According to the field distribution of the compressed cavity till meet the TE_{102} mode. We estimate the field strength of the compressed cavity by means of energy conservation.

Since the perturbation is located where the electric field is strongest, the magnetic field energy is ignored here. According to the energy conservation, we get the following formula,

$$E_0^2 \cdot a = E_c^2 \cdot d \tag{6}$$

Thus, the electric field strength at the compressed place of the compressed cavity can be estimated by as follow,

$$E_c = \sqrt{\frac{a}{d}} \cdot E_0 = \sqrt{\frac{8a^3(1 - \Gamma^2) \cdot P_{in} \cdot Q_c}{\varepsilon abd^3 \omega_0}} \tag{7}$$

Using equation (7), we can obtain the approximate electric field strength around the under testing materials.

III. EXPERIMENTAL SETUP

Based on the designed dual-mode compressed cavity, a physical model for studying the nonlinear interaction mechanism between microwave field and material is built up and shown in Fig. 4.

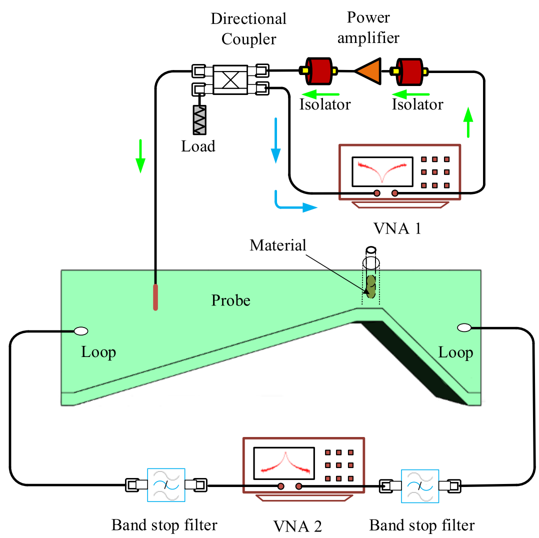

FIGURE 4. **Physical model for studying the nonlinear interaction mechanism between microwave field and material.**

The VNA 1 supplies a narrow band signals whose center frequency is around the TE_{102} mode and its power can be amplified by the amplifier continuously. The maximum output of the amplifier is about 53 dBm. The reflection between the VNA 1 and the amplifier is reduced by the two isolators. After being amplified, the stimulus signals are input into the compressed cavity through a probe, where presents a strong electric field. In order to ensure that the stimulus signal is input into the cavity, a directional coupler is used to extract the reflection signal. The reflection signal display on the VNA 1 by the transmission curve S21 and the power level of the stimulus signal that be input into the cavity (P_{in}) can be monitored by the the transmission curve S21. The testing signal is provided by the VNA 2, whose frequency is the same as that of the TE_{103} mode. Through the two loops, the testing signal is input into and coupled out of the cavity for measuring the dielectric performance of the materials under test. In addition, a high isolation between the two modes of the cavity can be achieved by the two band-stop filters with a more than total 60 dB attenuation in the stop band. The utilized experimental setup is shown in Fig. 5.

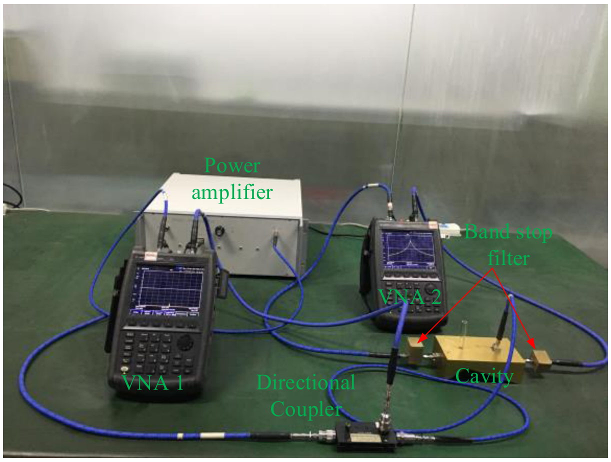

FIGURE 5. **The utilized experimental setup.**

In the experiment, a wide band signals with a very small power level (−40 dBm) is produced by VNA 1, firstly. The transmission curve is obtained on VNA 1. Search the minimum of the transmission curve of the VNA 1, and reset the output of the VNA 1 to a narrow band signal, whose center frequency is the minimum that we derived a moment ago. In this way, the energy of the stimulus signal is input into the cavity and TE_{102} mode and TE_{103} modes are excited. Meanwhile, the power level of the stimulus signals can be monitored at the same time.

IV. RESULTS AND DISCUSSION

In this paper, measurement is performed on InP, which is placed at the compressed part of the cavity. First of all, a low power level output signal (−40 dBm) with the working frequency derived according to the above method is given by the VNA 1. The transmission curve of the testing signal is obtained by the VNA 2, the black curve shown in Fig. 6. Then, the output of the VNA 1 is adjusted to 0 dBm and the transmission is acquired immediately, the red one shown in Fig. 6. The 0 dBm output power level of the VNA 1 is maintained for a few seconds. After that, change back the output power of the VNA 1 from 0 dBm to −40 dBm again, and the red transmission curve changes to the blue one right way as is shown in Fig. 6.

Fig. 6 distinctly illustrates that the resonant frequency has changed when the output power of the VNA 1 changes from −40 dBm to 0dBm. According to the cavity perturbation method [26], the real part of the dielectric constant results in the shift of resonant frequency, while the imaginary part causes the variation of the Q of the cavity, as is presented in equation (8) and (9). Therefore, the dielectric constant of InP is changed under the strong electric field. Furthermore, the blue curve is almost coincident with the black curve as depicted in Fig. 6, when the output power changes back to −40 dBm. This means that the nonlinear behavior of InP is not dominated by microwave heating but some other material

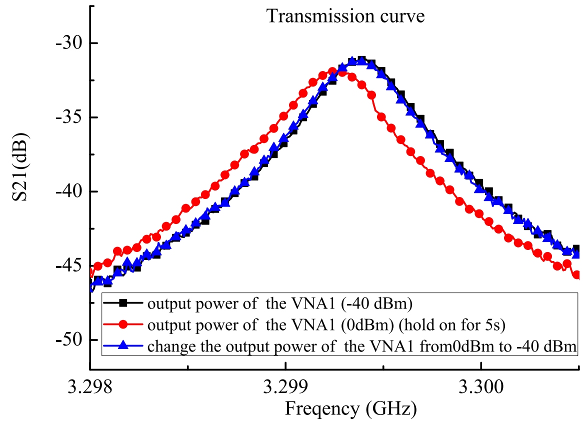

FIGURE 6. **Test curves of InP interacted with strong microwave field.**

inherent characteristics.

$$\frac{w - w_0}{w_0} = -\varepsilon_0(\varepsilon' - 1)\frac{\int_\Delta \vec{E} \cdot \vec{E_0}^* dV}{4W} \tag{8}$$

$$\frac{1}{Q} - \frac{1}{Q_0} = \varepsilon_0 \varepsilon'' \frac{\int_\Delta \vec{E} \cdot \vec{E_0}^* dV}{4W} \tag{9}$$

Where ω_0 and ω are the angular resonant frequency before and after the perturbation, respectively. Q_0 and Q are the quality factor with and without the test sample, respectively. $\vec{E}$ and $\vec{E_0}^*$ are the electric field vectors inside the perturbing sample and the unperturbed cavity, respectively. W is the total store energy in the cavity. And ε', ε'' are the real and imaginary parts of the dielectric constant.

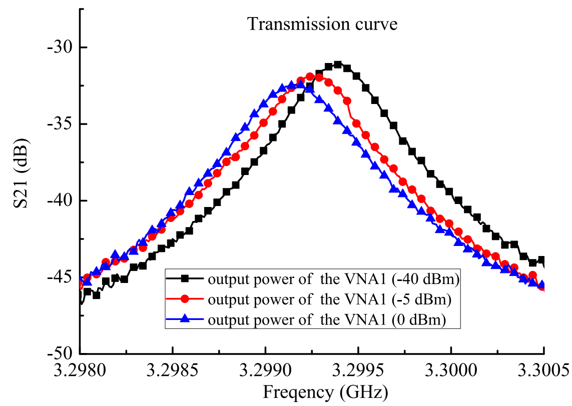

FIGURE 7. **Test curves of InP under different microwave field intensive.**

In Fig. 7, the three transmission curves are obtained under different strengths of microwave electric fields. The black one is obtained when the output of the VNA 1 is of −40 dBm. The red curve corresponds to the output of the VNA 1 is of −5 dBm, and the blue one is got when the output of the VNA 1 is of 0 dBm. It is easy to find that the dielectric property of the InP changes under those different microwave field strengths, even though the level of the changes is not the same. Additional observation has also been observed, the transmission curves remain stable when the microwave field strength did not exceed a critical value, however, after the microwave field strength exceeds the critical value, the non-linearity appears and the nonlinear behavior becomes more and more drastic along with the further increasing field strength.

In the experiment, the InP sample is loaded in a quartz tube to make the test easily. Therefore, it is necessary to exclude the influence of the quartz tube before the test. Fig. 8 show the experimental results of the quartz tube. The black curve and the red curve are obtained when the output signal is of −40 dBm and 0 dBm, respectively. It can be see that the black curve is entirely coincident with the red curve. That is to say, the dielectric property keep the same under given microwave field strength. Therefore, the quartz tube has no effect on our measurement processing and the nonlinear behavior observed in the experiment about InP is caused by the interaction between InP and microwave field.

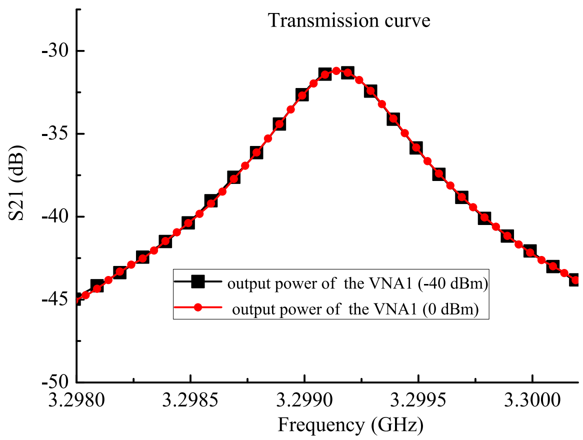

FIGURE 8. Measurement results of quartz tube under given different electric field.

To further investigate the nonlinearity of the InP, one more additional experiment is added. Firstly, set the VNA 1 output a wide band signal with a small power level (−40 dBm). Then, we can get the transmission curve S21 from the VNA 1 as is shown in Fig. 9 and it is actually the reflection of the stimulus signal. It is shown that only the narrow band frequency signal around 2.44 GHz is input into the cavity within one sweep time T. Search the minimum value of the transmission curve measured from the VNA 1, and reset the center frequency of the VNA1 to the frequency value corresponding to the minimum value of the previously searched transmission curve and the working bandwidth is 20 MHz. The sweep time T of the VNA 1 is set to 1.1s. In this way, the stimulus signal is similar to an impulse signals mode, and the time required to obtain a strong microwave electric field around the InP sample is much less than the sweep time T, eliminating the effect of the microwave thermal effects.

In order to monitor the dielectric property of the InP under different microwave electric field quickly, we only detect

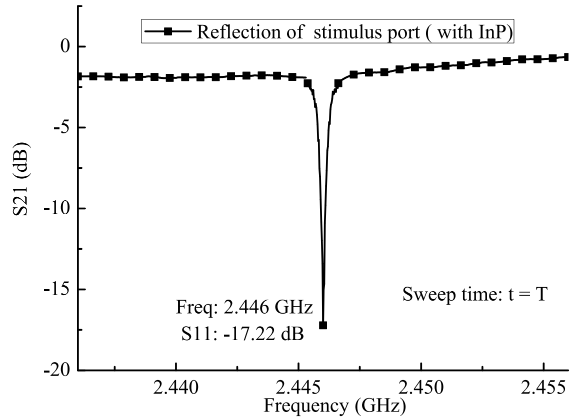

FIGURE 9. Reflection of the stimulus port with InP of the cavity.

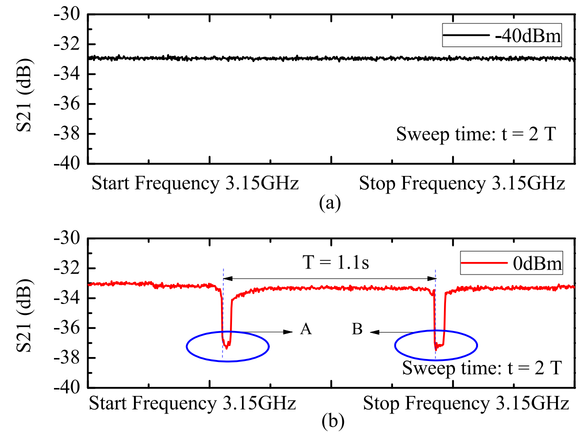

FIGURE 10. Test results of the InP. (a) test results obtained when the VNA 1 works with an output power of −40dBm and (b) test results when the VNA 1 works with an output power of −5dBm.

the resonant peak from VNA 2. Firstly, a wide band signals whose center frequency is around the resonant frequency of the mode TE_{103} are supplied by the VNA 2 and the transmission curve S21 is obtained by VNA 2. Search the maximum value of the curve and reset the sweep frequency range from the maximum value (the resonant peak point) to the maximum value, namely point frequency sweeping. The sweep time is set to 2 T.

Finally, the test results of the InP sample are obtained as shown in Fig. 10. Fig. 10 (a) and (b) shown the test results when the VNA 1 is working with a output power of −40 dBm, and −5 dBm, respectively. There are two special point (A and B) in Fig. 10 (b), which means the resonant peak has changes when the given power signals (−5 dBm) is input into the cavity. That's to say, the real part of the dielectric constant of the InP sample has changed under different microwave field strengths. According to the sweep time of the both VNAs, the sweep time of VNA 2 is two times of VNA 1, we can conclude that the nonlinear behavior is not caused by microwave thermal effect, but some inherent characteristics of material itself.

V. CONCLUSION

In this contribution, an experimental method and apparatus were introduced for investigating the interaction mechanism between microwave field and semiconductor material. During the experiment, some useful phenomena were obtained. Firstly, the dielectric property of InP changes under strong microwave field when the field strength exceeds a critical value. Secondly, the nonlinear dielectric is not dominated by the microwave heating but some other inherent property of the material itself. Thirdly, the speed of the appearance of the nonlinearity is related to the field strength. The stronger the microwave field strength is, the quicker the nonlinearity occurs. As far as we know, the nonlinearity is probably caused by a non-thermal microwave effects, which we think is associated with molecular polarizability. In addition, the experimental method and apparatus can also be employed to predict the consequences of non-thermal action of microwave effect of other high power microwave material under microwave filed.

REFERENCES

[1] J. R. Laghari and A. N. Hammoud, "A brief survey of radiation effects on polymer dielectrics," *IEEE Trans. Nucl. Sci.*, vol. 37, no. 2, pp. 1076–1083, Apr. 1990.

[2] G. Cheng and L. Liu, "Temporal evolution of multipactor electron discharge on a dielectric under excitation of high-power microwave," *IEEE Trans. Plasma Sci.*, vol. 39, no. 4, pp. 1067–1074, Apr. 2011.

[3] D. V. Korbutyak *et al.*, "Effect of microwave irradiation on the photoluminescence of bound excitons in CdTe:Cl single crystals," *Semiconductors*, vol. 45, no. 9, pp. 1133–1139, Sep. 2011.

[4] H. N. Raval, D. S. Sutar, P. R. Nair, and V. R. Rao, "Investigation of effects of ionizing radiation exposure on material properties of organic semiconducting oligomer—Pentacene," *Org. Electron.*, vol. 14, no. 6, pp. 1467–1476, Jun. 2013.

[5] G. Grainaru, T. S. Sudarshan, S. A. Gradinaru, W. Mitchell, and H. M. Hobgood, "Electrical properties of high resistivity 6H-SiC under high temperature/high field stress," *Appl. Phys. Lett.*, vol. 70, no. 6, pp. 735–737, Feb. 1997.

[6] M. Zielinski and M. Krzemieniewski, "The effect of microwave electromagnetic radiation on organic compounds removal efficiency in a reactor with a biofilm," *Environ. Technol.*, vol. 28, no. 1, pp. 41–47, May 2010.

[7] H. Liu, L. Guo, L. Zou, M. Cao, J. Zhou, and S. Ouyang, "Theoretical and experimental study on solid chemical reaction between $BaCO_3$ and TiO_2 in microwave field," *Mater. Sci. Eng. B*, vol. 113, no. 2, pp. 161–165, Jul. 2004.

[8] R. K. Ahrenkiel and W. Johnston, "Interaction of microwaves with photoelectrons in semiconductors," *J. Vac. Sci. Technol. B, Microelectron. Process. Phenom.*, vol. 26, no. 4, pp. 1508–1515, Aug. 2008.

[9] A. Kozyrev, A. Ivanov, T. Samoilova, O. Soldatenkov, K. Asrafiev, and L. C. Sengupta, "Nonlinear response and power handling capability of ferroelectric $Ba_xSr_{1-x}TiO_3$ film capacitors and tunable microwave devices," *J. Appl. Phys.*, vol. 88, no. 9, pp. 5334–5342, Nov. 2000.

[10] E. Gaganidze, R. Heidinger, J. Halbritter, A. Shevchun, M. Trunin, and H. Schneidewind, "Nonlinear surface impedance of $Tl_2Ba_2CaCu_2O_8$ thin films as a function of temperature, frequency, and magnetic field," *J. Appl. Phys.*, vol. 93, no. 7, pp. 4049–4054, 2003.

[11] T. Feng, H. Ding, D. Gao, and Z. Zhang, "Numerical simulation and experiment of hardening behaviors in unsaturated polyester resin artificial marble blocks under microwave radiation," *IEEE Trans. Plasma Sci.*, vol. 44, no. 10, pp. 2485–2492, Oct. 2016.

[12] J. Krupka, J. G. Hartnett, and M. Piersa, "Permittivity and microwave absorption of semi-insulating InP at microwave frequencies," *Appl. Phys. Lett.*, vol. 98, no. 11, p. 112112, Mar. 2011.

[13] A. S. Semisalova, N. S. Perov, G. V. Stepanov, E. Y. Kramarenkoa, and A. R. Khokhlova, "Strong magnetodielectric effects in magnetorheological elastomers," *Soft Matter*, vol. 9, no. 47, pp. 11318–11324, 2013.

[14] O. Soldatenkov, T. Samoilova, A. Ivanov, A. Kozyrev, D. Ginley, and T. Kaydanova, "Nonlinear properties of thin ferroelectric film-based capacitors at elevated microwave power," *Appl. Phys. Lett.*, vol. 89, no. 23, p. 232901, Dec. 2006.

[15] H. Wang, W. Wang, Q. Gong, and S. Wang, "External electric field effect on exciton binding energy in InGaAsP/InP cylindrical quantum wires," *Phys. B, Condens. Matter*, vol. 503, no. 9, pp. 117–120, Sep. 2016.

[16] F. Komarov, P. Gaiduk, and A. Kamarou, "Damage evolution and track formation in crystalline InP and GaAs during swift Kr and Xe ion irradiation," *Vacuum*, vol. 63, no. 4, pp. 657–663, Mar. 2001.

[17] A. Kamarou, E. Wendler, and W. Wesch, "Charge state effect on near-surface damage formation in swift heavy ion irradiated InP," *J. Appl. Phys.*, vol. 97, no. 12, p. 123532, Jun. 2005.

[18] R. L. Dubey, S. K. Dubey, A. D. Yadav, and D. Kanjilal, "Surface modification of indium phosphide by 100 MeV iron ions," *Radiat. Effects Defects Solids*, vol. 168, nos. 7–8, pp. 557–563, Mar. 2013.

[19] A. Y. Didyk and A. S. Khalil, "Properties of indium phosphite and selected compounds under irradiation with swift heavy ions," *Phys. Part. Nucl.*, vol. 41, no. 2, pp. 230–284, Feb. 2010.

[20] M. Yamaguchi, T. Takamoto, and M. Ohmori, "Analysis of the anomalous spectral response of InP solar cells induced by high fluence proton irradiation," *J. Appl. Phys.*, vol. 83, no. 3, pp. 1116–1119, Feb. 1997.

[21] H.-Y. Kim, C. F. Lo, L. Liu, F. Ren, J. Kim, and S. J. Pearton, "Proton-irradiated InAlN/GaN high electron mobility transistors at 5, 10, and 15 MeV energies," *Appl. Phys. Lett.*, vol. 100, no. 1, pp. 012107-1–012107-3, Jan. 2012.

[22] A. A. Belyaev *et al.*, "Influence of microwave treatment on the electrophysical characteristics of technically important semiconductors and surface-barrier structures," *Tech. Phys.*, vol. 43, no. 12, pp. 1445–1449, Dec. 1998.

[23] G. I. Ovchinnikova, Y. A. Pirogow, N. A. Bobkov, N. V. Belugina, R. V. Gainutdinov, and A. L. Tolatikhina, "AFM investigation of the mechanism for microwave effect on ferroelectric triglycine sulfate," *Phys. Wave Phenomena*, vol. 21, no. 1, pp. 52–55, Jan. 2013.

[24] N. S. Zayats, R. V. Konakova, V. V. Milenin, G. V. Milenin, R. A. Red'ko, and S. N. Red'ko, "Microwave-radiation-induced structural transformations in homo- and heterogeneous GaAs-based systems," *Tech. Phys.*, vol. 60, no. 3, pp. 432–436, Mar. 2014.

[25] D. M. Pozar, *Microwave Engineering*, 3rd ed. Amherst, MA, USA: Electronics Industry, 2005, pp. 278–279.

[26] A. Kik, "Complex permittivity measurement using a ridged waveguide cavity and the perturbation method," *IEEE Trans. Microw. Theory Techn.*, vol. 64, no. 11, pp. 3878–3886, Nov. 2016.

YONG GAO received the B.Sc. degree in electronic information engineering from Anhui Normal University, Wuhu, China, in 2012, where he is currently pursuing the Ph.D. degree in electromagnetic fields and microwave technology from the University of Electronic Science and Technology of China, Chengdu, China, in 2017. His research interests include nonlinear dielectric properties of high power microwave material, high power devices feature parameter extraction, passive intermodulation test technology, design of microwave devices, and microwave integrated circuits.

EN LI (M'17) received the M.S. degree in physical electronics and the Ph.D. degree in electromagnetic field and microwave technology from the University of Electronic Science and Technology of China, Chengdu, China, in 2003 and 2009, respectively. In 1997, he joined the University of Electronic Science and Technology of China, as a Faculty Member. From 2005 to 2010, he was an Associate Professor , and he was involved in research projects in the areas of electro-magnetic parameters measurement of materials, design of microwave device design, and automatic microwave test system. Since 2010, he has been a Professor, and he has taken charge of the research projects in the areas of electromagnetic parameters measurement of dielectric materials at high temperatures and microwave plasma diagnosis. He has authored or co-authored over 100 journal and conference papers. He holds 19 authorized national invention patents. His current main research interests include microwave plasma diagnosis, electromagnetic parameter measurement of dielectric material at high temperatures, nonlinear parameter measurement of high power amplifier, and design of microwave devices. He is a Guest Professor of the National Defense Science and Technology Key Lab of Advanced Function Composite Material and a member of the Standing Council of the National Materials New Technology Development Research Institute. He was a recipient of the Second Prize of the National Science and Technology Progress Award and the First Prize, the Second Prize, and the Third Prize of provincial and ministerial level scientific and technological progress awards. He was a recipient of the title of ''Excellent Experts'' with outstanding contribution of Sichuan Province in 2013. He was a Winner of the Education Ministry's New Century Excellent Talents Supporting Plan in 2010. He was a Reserve Candidate of Academic and Technical Leader of Sichuan Province in 2013.

GAOFENG GUO received the M.S. and Ph.D. degrees in physical electronics from the University of Electronic Science and Technology of China, Chengdu, China, in 2000 and 2008, respectively. In 2000, she joined the University of Electronic Science and Technology of China, as a Faculty Member. From 2001 to 2006, she was a Lecturer, and she was involved with research projects in the area of electromagnetic parameter measurement of microwave dielectric material. Since 2006, she has been an Associate Professor, and she has been involved in research projects in the areas of electromagnetic parameters measurement of dielectric materials and dielectric property measurement at high temperatures. Her current research interests include electromagnetic parameter measurement of dielectric material and nonlinear parameter measurement of high power amplifier.

HU ZHENG received the M.S. degree in optics from Xidian University, Xi'an, China, in 2005, and the Ph.D. degree in electronic engineering from the University of Chinese Academy of Sciences, Beijing, China, in 2008. He is currently an Associate Professor with the University of Electronic Science and Technology of China. His current research focuses on microwave imaging, indirect holography, microwave measurement theory, nonlinear dielectric of microwave material, and nonlinear measurement.